

## Surface plasmon resonances of protein-conjugated gold nanoparticles on graphitic substrates

Anh D. Phan, Trinh X. Hoang, Thi H. L. Nghiem, and Lilia M. Woods

Citation: *Appl. Phys. Lett.* **103**, 163702 (2013); doi: 10.1063/1.4826514

View online: <http://dx.doi.org/10.1063/1.4826514>

View Table of Contents: <http://apl.aip.org/resource/1/APPLAB/v103/i16>

Published by the [AIP Publishing LLC](#).

---

### Additional information on *Appl. Phys. Lett.*

Journal Homepage: <http://apl.aip.org/>

Journal Information: [http://apl.aip.org/about/about\\_the\\_journal](http://apl.aip.org/about/about_the_journal)

Top downloads: [http://apl.aip.org/features/most\\_downloaded](http://apl.aip.org/features/most_downloaded)

Information for Authors: <http://apl.aip.org/authors>



## Re-register for Table of Content Alerts

Create a profile.



Sign up today!



# Surface plasmon resonances of protein-conjugated gold nanoparticles on graphitic substrates

Anh D. Phan,<sup>1,2,a)</sup> Trinh X. Hoang,<sup>2</sup> Thi H. L. Nghiem,<sup>2</sup> and Lilia M. Woods<sup>1</sup>

<sup>1</sup>Department of Physics, University of South Florida, Tampa, Florida 33620, USA

<sup>2</sup>Institute of Physics, 10 Dao Tan, Badih, Hanoi, Vietnam

(Received 28 May 2013; accepted 8 October 2013; published online 17 October 2013)

We present theoretical calculations for the absorption properties of protein-coated gold nanoparticles on graphene and graphite substrates. As the substrate is far away from nanoparticles, numerical results show that the number of protein bovine serum molecules aggregating on gold surfaces can be quantitatively determined for gold nanoparticles with arbitrary size by means of the Mie theory and the absorption spectra. The presence of a graphene substrate near the protein-conjugated gold nanoparticles results in a red shift of the surface plasmon resonances of the nanoparticles. This effect can be modulated upon changing the graphene chemical potential. Our findings show that the graphene and graphite affect the absorption spectra in a similar way. © 2013 AIP Publishing LLC. [<http://dx.doi.org/10.1063/1.4826514>]

The enhancement of surface interactions and quantum confinement effects are at the heart of many novel applications at the nanoscale. Of particular interest are magnetic nanoparticles (NPs). While NPs made of Fe<sub>3</sub>O<sub>4</sub> or Co show novel magnetic characteristics strongly sensitive to external fields, noble metal NPs, made of Au, have fascinating properties derived from their localized surface plasmon resonances. Consequently, NPs have been used in a variety of devices, such as solar cells,<sup>1–3</sup> electrocatalysts,<sup>4</sup> and sensors with high sensitivity.<sup>5–7</sup> In many applications, the support of substrates to metallic NPs are proven to be highly effective in maximizing the performance of these structures.<sup>8–12</sup> One of the interesting features due to the presence of a substrate is the red shift in the resonance wavelength. This effect is strong in metallic NPs and it is particularly useful for the design of optical sensors.

Gold nanoparticle bioconjugates have also been investigated in order to construct functional devices for cellular imaging, drug delivery, and biomolecule detection. Bovine Serum Albumin (BSA) proteins have been particularly useful in this regard.<sup>13</sup> The BSA substance not only prevents the AuNPs to assemble together but it is also effective for therapeutic deliveries and attaching AuNPs in living matter. Because of their large scattering cross sections, individual BSA-AuNPs can be imaged under white light illumination. Furthermore, finding ways to tune the plasmon resonances across the visible spectrum via changing the particle size and shape has been particularly useful in optimizing the application of nanoparticles bioconjugates.

Graphene, an atomically thin 2D material, with outstanding mechanical, optical, and electric properties has been broadly investigated as a promising support material for metallic NPs.<sup>8–10,14</sup> In theoretical studies, researchers used the dielectric function of pristine graphene fitted from available experimental data.<sup>15</sup> However, such modelling has limitations since it cannot take into account the effect of doping, external fields, and temperature in a continuous way.

Previous studies have shown that these factors can be used effectively to tune the response properties of graphene for a variety of applications

In this paper, the absorption and scattering cross sections of a AuNP in an aqueous BSA protein solution on a graphitic substrate (Fig. 1) is considered theoretically. The system is formed as the BSA protein and AuNP are placed in water. Some of the water mixes with the protein, and this BSA aqueous solution is attracted to the AuNP via a van der Waals interaction (Fig. 1(a)). As a result, a protein conjugated nanoparticle is formed in the water. The composite particle is positioned above a graphitic substrate, as shown in Fig. 1(b). For the calculations, the Mie theory is used via the expressions<sup>16</sup>

$$\begin{aligned}\sigma_{sca} &= \frac{k^4}{6\pi} |\alpha|^2, \\ \sigma_{abs} &= k \text{Im}(\alpha),\end{aligned}\quad (1)$$

where  $\sigma_{sca}$  and  $\sigma_{abs}$  correspond to the scattering and absorption spectra of the system, respectively. Also,  $\alpha$  is the resultant polarizability of the objects,  $k = 2\pi n/\lambda$ , and  $n$  is the refractive index of medium.

The core-shell particle without the graphene (Fig. 1(b)) is considered first ( $d = \infty$ ). The composite polarizability is found from Maxwell-Garnett (MG) theory for an effective medium approximation<sup>17</sup>

$$\alpha = 4\pi r_2^3 \frac{\epsilon_2 \epsilon_a - \epsilon_3 \epsilon_b}{\epsilon_2 \epsilon_a + 2\epsilon_3 \epsilon_b}, \quad (2)$$

$$\epsilon_a = \epsilon_1 \left[ 1 + 2 \left( \frac{r_1}{r_2} \right)^3 \right] + 2\epsilon_2 \left[ 1 - \left( \frac{r_1}{r_2} \right)^3 \right], \quad (3)$$

$$\epsilon_b = \epsilon_1 \left[ 1 - \left( \frac{r_1}{r_2} \right)^3 \right] + \epsilon_2 \left[ 2 + \left( \frac{r_1}{r_2} \right)^3 \right], \quad (4)$$

where  $\epsilon_1$ ,  $\epsilon_2$ , and  $\epsilon_3$  are the dielectric function for the core (AuNP), shell (BSA), and surrounding medium, respectively.

<sup>a)</sup>Electronic mail: [anhphan@mail.usf.edu](mailto:anhphan@mail.usf.edu)

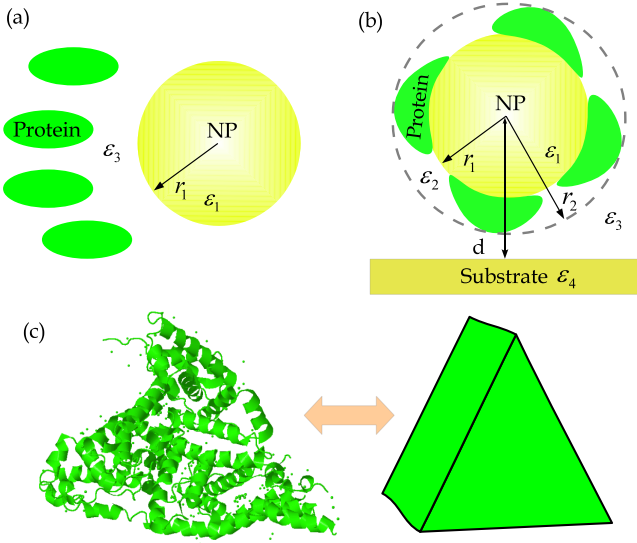


FIG. 1. (a) BSA protein adsorbing on an AuNP. (b) Schematic illustration of AuNP and a substrate at a separation distance  $d$  measured from the center of NP to the surface of the substrate. (c) BSA protein modelled by an equilateral triangular prism with dimensions  $84 \times 84 \times 84 \times 31.5 \text{ \AA}$ .

The dielectric function for the Au core can be described by a Drude model  $\epsilon_1 = 1 - \omega_p^2 / [\omega(\omega + i\Gamma)]$  with  $\omega_p$  being the plasma frequency of gold and  $\Gamma$  being the damping parameter. We note that the Drude expression works well for bulk predicting a plasmon resonance at around 216 nm.<sup>17</sup> However, for AuNP with diameter of 15 nm, the resonant wavelength is observed at around 510 nm.<sup>18</sup> This shift has been attributed to the finite size of the nanoparticles. Other experimental data show that the Drude model is not sufficient to describe the Au dielectric properties for a wider frequency range.<sup>19</sup>

To accommodate wider frequency range and take into account the dimensions of the AuNP, we use a modified Drude-Lorentz model with several oscillators<sup>20</sup>

$$\epsilon_1(\lambda) = 1 - \frac{f_0/\lambda_p^2}{1/\lambda^2 + i/(\lambda\gamma_0)} + \sum_{j=1}^5 \frac{f_j/\lambda_p^2}{1/\lambda_j^2 - i/(\lambda\gamma_j) - 1/\lambda^2}, \quad (5)$$

in which  $f_0$  and  $f_j$  are the oscillator strengths. The first two terms in Eq. (5) represent the Drude term in the Au dielectric function with modified plasma frequency due to  $f_0$ . The other terms correspond to interband transitions from the bound electrons. The Au dielectric function has been obtained experimentally and it can be represented via five oscillators with a very good accuracy. The experimental characteristics, typically given in terms of wavelengths ( $\lambda_{p,i} = 2\pi c/\omega_{p,i}$ ), are shown in Table I.

The finite size of the nanoparticle is particularly important when  $r_1 \leq 20$  nm. Its effect is taken into account by modifying the scattering parameter  $\gamma = \gamma_0 + A v_F / r_1$ , where  $v_F$  is the Au Fermi velocity<sup>19</sup> and  $0.1 \leq A \leq 1$  is the parameter describing the scattering processes.<sup>19</sup> Clearly, if  $A$  is large and  $r_1$  is small,  $\gamma$  can differ significantly from the bulk  $\gamma_0$ .

Since the protein is in water solution, the dielectric function of the BSA/water mixture is described as a composite given by

TABLE I. Parameters for dielectric function of AuNP and graphite provided in Refs. 20 and 21.

Parameter	AuNP	Graphite
$f_0$	0.76	0.014
$\gamma_0$ (nm)	23438.9	195.17
$\lambda_p$ (nm)	138	46.01
$f_1$	0.024	0.073
$\gamma_1$ (nm)	5154.6	302.84
$\lambda_1$ (nm)	2993.4	4517.31
$f_2$	0.010	0.056
$\gamma_2$ (nm)	3600.75	169.52
$\lambda_2$ (nm)	1496.7	354.122
$f_3$	0.071	0.069
$\gamma_3$ (nm)	418.41	878.54
$\lambda_3$ (nm)	1427.9	279.10
$f_4$	0.601	0.005
$\gamma_4$ (nm)	498.1	27005.65
$\lambda_4$ (nm)	288.63	91.403
$f_5$	4.384	0.262
$\gamma_5$ (nm)	561.1	667.164
$\lambda_5$ (nm)	93.26	87.323
$f_6$	...	0.460
$\gamma_6$ (nm)	...	104.2
$\lambda_6$ (nm)	...	15.55
$f_7$	...	0.2
$\gamma_7$ (nm)	...	31.78
$\lambda_7$ (nm)	...	38.81

$$\epsilon_2(\lambda) = f\epsilon_{protein} + (1-f)\epsilon_w, \quad (6)$$

where  $f$  is the fraction of protein comprising the shell and  $\epsilon_w = 1.77$  is the dielectric constant of water.<sup>19</sup> BSA can also be described via a set of Lorentz oscillators<sup>22</sup>

$$\epsilon_{protein}(\lambda) = 1 + \sum_j \frac{1/\Lambda_j^2}{1/\lambda_j^2 - i/(\lambda\gamma_j) - 1/\lambda^2}. \quad (7)$$

Experimental studies have shown that the BSA spectrum can be accurately represented with four oscillators with characteristics given  $\Lambda_1 = 10853.54$  nm,  $\Lambda_2 = 878.5$  nm,  $\Lambda_3 = 92.6$  nm,  $\Lambda_4 = 82.81$  nm,  $\gamma_1 = \infty$ ,  $\gamma_2 = 2484.52$  nm,  $\gamma_3 = 155.28$  nm,  $\gamma_4 = 65.38$  nm,  $\lambda_1 = 6059.8$  nm,  $\lambda_2 = 194.1$  nm,  $\lambda_3 = 99.38$  nm, and  $\lambda_4 = 57.78$  nm.<sup>22</sup>

The medium is taken to be water with a dielectric function  $\epsilon_3 = \epsilon_w$ .

The absorption and scattering sections for the cases of AuNP without and with the BSA layer submerged in water are calculated. The results presented in Figure 2 show how  $\sigma_{abs,scatt}$  behaves as a function of the wavelength. Here, we take that  $r_1 = 8$  nm for the AuNP and  $r_2 = 11.15$  nm for the shell. Recent experiments indicate that such a configuration corresponds to a BSA monolayer around the Au core.<sup>23</sup> To achieve a very good agreement with the reported data in Ref. 18 for the AuNP/water system, the parameter  $A$ , which takes into account the finite size of the NP in  $\gamma_0$ , is taken to be  $A = 0.4$ . For the case of AuNP/BSA/water,  $A = 0.61$ .<sup>19,24</sup> The increase in  $A$  indicates that the presence of the protein enhances the effect of the finite NP size on the cross section. Figure 2(a) shows that the absorption spectrum has similar

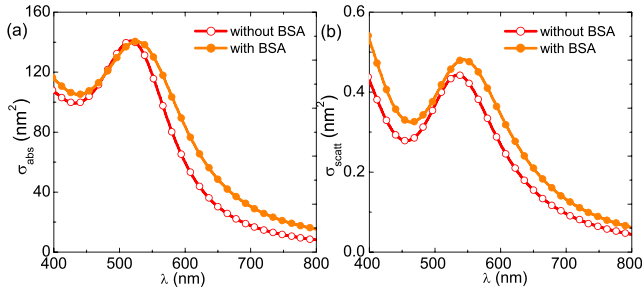


FIG. 2. The absorption and scattering cross sections of AuNPs in water with and without BSA in the visible spectrum. The diameter of AuNPs in the calculations is 16 nm.

magnitude regardless of the presence of BSA, although the protein reduces the width of the peak to some extent. It is clear that by changing  $A$ , one can modify  $\sigma_{abs}$ . Figure 2 also indicates that the spectrum is dominated by absorption as  $\sigma_{scatt}$  is several orders of magnitude smaller as compared to  $\sigma_{abs}$ . Thus, for the rest of this study, only the absorption spectrum is considered.

The parameter  $f$  in Eq. (6) characterizing the fraction of BSA present in the shell also affects the absorption and scattering spectra. Figure 2 illustrating plasmon shifts of AuNPs in aqueous environment due to adding BSA proteins can be explained by taking  $f=0.4$ . We can employ this model to explain surface plasmon absorption shifts if DNA is added to the aqueous solution instead of BSA proteins.<sup>25</sup> Further studies investigating NPs of various shapes and extensions<sup>26,27</sup> show that the size of the NPs have a much greater effect on the spectra, while  $f \approx 0.4$ . Since the  $f$  value is directly related to amount of protein around the core, it is concluded that a single layer of protein forms the shell regardless of NP dimensions.<sup>23,24,27</sup> Thus, based on this, we take  $f=0.4$  for the calculation presented here.

In addition to examining the absorption spectrum of Au NPs and the role of BSA, the number of proteins in the shell can also be estimated using

$$N = \frac{4\pi f(r_2^3 - r_1^3)}{3V_0}, \quad (8)$$

where  $V_0$  is the volume of one BSA protein molecule. Several studies have shown that BSA conforms into a heart-like shaped structure<sup>23,28,29</sup> sketched in Fig. 1(c) surrounding the AuNP. Here, we model this with triangular shape with equal sides of 84 Å and thickness of 31.5 Å. Using Eq. (8), it is found that  $N \approx 15$ , which compares well with the previous experiments,<sup>23</sup> which report  $N \approx 12$  BSA protein molecules around a AuNP with an average diameter of 13 nm. Another previous paper<sup>27</sup> reported that there are approximately 16 BSA molecules on the AuNPs with diameter 15 nm because the surface density of protein BSA is  $2 \times 10^{12}$  molecules/cm<sup>2</sup> for AuNPs with the diameter of 10–20 nm. As a result, our calculation has a good agreement with previous experiments studies. One notes that the number of proteins increases linearly with the radius of the NP. In practical, it is difficult to synthesize all NPs with the same size. It was found that the size effects have a considerable impact on the optical response of NP.<sup>26</sup> Individual metallic

NPs with desired shape and size with attached BSA proteins can be characterized using optical trapping.<sup>30,31</sup>

We further investigate how the protein covered AuNP absorption spectrum is affected by the presence of a substrate. In this case, the polarizability of the nanoparticle is modified according to<sup>32</sup>

$$\alpha_m = \alpha \left[ 1 - \left( \frac{r_2}{2d} \right)^3 \frac{\varepsilon_2 \varepsilon_a - \varepsilon_3 \varepsilon_b}{\varepsilon_2 \varepsilon_a + 2\varepsilon_3 \varepsilon_b} \frac{\varepsilon_4 - \varepsilon_3}{\varepsilon_4 + \varepsilon_3} \right]^{-1}, \quad (9)$$

where  $\varepsilon_4$  is the dielectric function of the substrate and  $d$  is the distance between the center of AuNP and the surface of substrate. For most materials, it is not easy to modify the response properties in a continuous and controlled manner. Being able to modulate  $\varepsilon_4$  in such fashion can be beneficial for the optical control of the AuNP/protein composites to devise efficient ways for biosensing with high sensitivity. Recent work has shown that response properties of graphene can be tuned via its chemical potential  $\mu$ .<sup>33,34</sup> Doping or applied external electric fields can change  $\mu$ , which affects its surface plasmon characteristics.

Here, we consider graphene and graphite as two possible substrates. Our goal is to provide an effective way to change the surface plasmon characteristics of the core-shell structures by manipulating the substrate. In addition, we will distinguish the role of the surface of the substrate as compared to the bulk.

To facilitate our studies, the graphene dielectric function is calculated via the 2D conductivity  $\sigma$ , which is expressed using the Kubo formalism with the chemical potential  $\mu$  explicitly taken into account<sup>35</sup>

$$\varepsilon_4(\omega) = \varepsilon_g(\omega) = 1 + \frac{i\sigma(\omega)}{\varepsilon_0 \omega h_0}, \quad (10)$$

$$\sigma(\omega) = \frac{2ie^2 k_B T}{\pi \hbar^2 \omega} \ln \left( 2 \cosh \frac{\mu}{2k_B T} \right) + \frac{e^2}{4\hbar} \left[ \theta(\hbar\omega - 2\mu) - \frac{i}{2\pi} \ln \frac{(\hbar\omega + 2\mu)^2}{(\hbar\omega - 2\mu)^2} \right], \quad (11)$$

where  $h_0 = 0.34$  nm is the thickness of graphene,  $\varepsilon_0$  is the vacuum permittivity,  $k_B$  is the Boltzmann constant,  $T$  is temperature,  $\hbar$  is the Plank constant, and  $e$  is the charge of electron. Note that Eq. (11) is valid when  $\mu \gg k_B T$ . For pristine graphene ( $\mu = 0$ ), the graphene conductivity is described via its universal value  $\sigma(\omega) = \sigma_0 = e^2/4\hbar$ .<sup>35</sup> The chemical potential of graphene can be easily changed via an applied external electric field. Using the relation<sup>33,34</sup>  $\frac{\pi \varepsilon_0 \hbar^2 v_0^2}{e} \mathbb{E} = \int_0^\infty E [f(E) - f(E + 2\mu)] dE$  with  $v_0 = c/300$ , one finds, for example, that electric field of strength  $\mathbb{E} = 6.64 \times 10^9$  V/m corresponds to  $\mu = 1$  eV at  $T = 300$  K.

The dielectric function for graphite  $\varepsilon_4(\omega) = \varepsilon_g(\omega)$  can be calculated via Eq. (5) with characteristics shown in Table I. These have been calculated via *ab initio* simulations and also compared to available experimental data to ensure that they reproduce well the dielectric and optical properties of graphite.<sup>21,36</sup>

The calculated absorption spectra of the BSA conjugated AuNP in aqueous solution above a graphene substrate

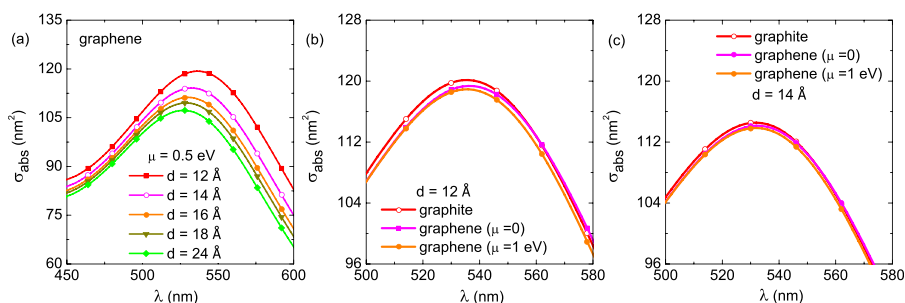


FIG. 3. The absorption cross section of protein-coated AuNPs in an aqueous solution on (a) graphene substrate with  $\mu = 0.5$  eV with different value of  $d$ , (b) graphite, pristine graphene and graphene with  $\mu = 1$  eV at  $d = 12$  Å, and (c) graphite, pristine graphene, and graphene with  $\mu = 1$  eV at  $d = 14$  Å.

is shown in Fig. 3(a) for different NP/graphene separations. It appears that only an absorption maximum is found here, which is different than the absorption maximum and minimum without the presence of graphene (Fig. 2(a)). As the substrate is brought closer to the NP, the absorption cross section increases with its maximum shifting towards larger  $\lambda$  values. For example, the surface plasmon frequency is at 536.4 nm for  $d = 12$  Å and 527 nm at 24 nm. We also find that the plasmon does not change significantly for  $d \geq 25$  nm, thus, one can conclude that the NP is not affected by the graphene in a significant way.

Figs. 3(b) and 3(c) also show that substituting graphene by graphite hardly affects  $\sigma_{abs}$ . The relatively small shifts (0.1 nm) of the resonance peaks are difficult to detect with available experimental techniques. Thus, the absorption is influenced only by the graphene layer closest to the NP.

In conclusion, we have studied the optical properties of BSA protein wrapped around AuNPs in aqueous solution. Our calculations show that a graphene substrate can introduce experimentally observable shifts in the plasmon spectra. The ability to influence the graphene response properties via a chemical potential provides a beneficial way to tune the optical properties of the nanoparticles. We also show that the finite size of the nanoparticles can play a significant role in the plasmon spectra shifts, and it is directly related to the number of protein molecules attached to the AuNP surface. Estimating the number of protein molecules can help the analysis of experimental data since such measurements are challenging for current techniques.

We gratefully acknowledge helpful discussions with Professor Onofrio M. Marago. This work was supported by the Nafosted Grant No. 103.01-2013.16. Lilia M. Woods acknowledges the Department of Energy under Contract No. DE-FG02-06ER46297.

- <sup>1</sup>J. Yang, J. You, C. C. Chen, W. C. Hsu, H. R. Tan, X. W. Zhang, Z. Hong, and Y. Yang, *ACS Nano* **5**, 6210 (2011).
- <sup>2</sup>S. Pillai, K. R. Catchpole, T. Trupke, and M. A. Green, *J. Appl. Phys.* **101**, 093105 (2007).
- <sup>3</sup>B. Cai, B. Jia, Z. Shi, and M. Gu, *Appl. Phys. Lett.* **102**, 093107 (2013).
- <sup>4</sup>M. M. Schubert, S. Hackenberg, A. C. van Veen, M. Muhler, V. Plzak, and R. J. Behm, *J. Catal.* **197**, 113 (2001).
- <sup>5</sup>A. J. Haes and R. P. Van Duyne, *J. Am. Chem. Soc.* **124**, 10596 (2002).
- <sup>6</sup>J. Devkota, C. Wang, A. Ruiz, S. Mohapatra, P. Mukherjee, H. Srikanth, and M. H. Phan, *J. Appl. Phys.* **113**, 104701 (2013).

- <sup>7</sup>J. Devkota, A. Ruiz, P. Mukherjee, H. Srikanth, and M. H. Phan, *IEEE Trans. Magn.* **49**, 4060 (2013).
- <sup>8</sup>T. Wu, J. Ma, X. Wang, Y. Liu, H. Xu, J. Gao, W. Wang, Y. Liu, and J. Yan, *Nanotechnology* **24**, 125301 (2013).
- <sup>9</sup>W. Hong, H. Bai, Y. Xu, Z. Yao, Z. Gu, and G. Shi, *J. Phys. Chem. C* **114**, 1822 (2010).
- <sup>10</sup>J. Jasuja, L. Linn, S. Melton, and V. Berry, *J. Phys. Chem. Lett.* **1**, 1853 (2010).
- <sup>11</sup>G. V. Bianco, M. M. Giangregorio, M. Losurdo, P. Capezzuto, and G. Bruno, *Adv. Funct. Mater.* **22**, 5081 (2012).
- <sup>12</sup>K. Qadir, S. H. Kim, S. M. Kim, H. Ha, and J. Y. Park, *J. Phys. Chem. C* **116**, 24054 (2012).
- <sup>13</sup>S. Lal, S. E. Clare, and J. Halas, *Acc. Chem. Res.* **41**, 1842 (2008).
- <sup>14</sup>J. Niu, Y. J. Shin, Y. Lee, J.-H. Ahn, and H. Yang, *Appl. Phys. Lett.* **100**, 061116 (2012).
- <sup>15</sup>V. G. Kravets, A. N. Grigorenko, R. R. Nair, P. Blake, S. Anissimova, K. S. Novoselov, and A. K. Geim, *Phys. Rev. B* **81**, 155413 (2010).
- <sup>16</sup>A. Housni, M. Ahmed, S. Liu, and R. Narain, *J. Phys. Chem. C* **112**, 12282 (2008).
- <sup>17</sup>C. F. Bohren and D. R. Huffman, *Absorption and Scattering of Light by Small Particles* (Wiley, Weinheim, Germany 1998).
- <sup>18</sup>O. Muskens, D. Christofilos, N. D. Fatti, and F. Vallee, *J. Opt. A: Pure Appl. Opt.* **8**, S264 (2006).
- <sup>19</sup>V. Amendola and M. Meneghetti, *J. Phys. Chem. C* **113**, 4277 (2009).
- <sup>20</sup>A. D. Rakic, A. B. Djuricic, J. M. Elazar, and M. L. Majewski, *Appl. Opt.* **37**, 5271 (1998).
- <sup>21</sup>A. B. Djuricic and E. H. Li, *J. Appl. Phys.* **85**, 7404 (1999).
- <sup>22</sup>C. M. Roth, B. L. Neal, and A. M. Lenhoff, *Biophys. J.* **70**, 977 (1996).
- <sup>23</sup>D.-H. Tsai, F. W. DelRio, A. M. Keene, K. M. Tyner, R. I. MacCuspie, T. J. Cho, M. R. Zachariah, and V. A. Hackley, *Langmuir* **27**, 2464 (2011).
- <sup>24</sup>T. H. L. Nghiem, T. H. La, X. H. Vu, V. H. Chu, T. H. Nguyen, Q. H. Le, E. Fort, Q. H. Do, and H. N. Tran, *Adv. Nat. Sci.: Nanosci. Nanotechnol.* **1**, 025009 (2010).
- <sup>25</sup>P. K. Jain, W. Qian, and M. A. El-Sayed, *J. Am. Chem. Soc.* **128**, 2426 (2006).
- <sup>26</sup>S. Link and M. A. El-Sayed, *J. Phys. Chem. B* **103**, 4212 (1999).
- <sup>27</sup>J. H. Teichroeb, J. A. Forrest, and L. W. Jones, *Eur. Phys. J. E* **26**, 411 (2008).
- <sup>28</sup>M. L. Ferrer, R. Duchowicz, B. Carrasco, J. G. de la Torre, and A. U. Acuna, *Biophys. J.* **80**, 2422 (2001).
- <sup>29</sup>C. Rocker, M. Potzl, F. Zhang, W. J. Parak, and G. U. Nienhaus, *Nat. Nanotechnol.* **4**, 577 (2009).
- <sup>30</sup>E. Messina, E. Cavallaro, A. Cacciola, R. Saija, F. Borghese, P. Denti, B. Fazio, C. D. Andrea, P. G. Gucciardi, M. A. Iati *et al.*, *J. Phys. Chem. C* **115**, 5115 (2011).
- <sup>31</sup>R. Saija, P. Denti, F. Borghese, O. M. Marago, and M. A. Iati, *Opt. Express* **17**, 10231 (2009).
- <sup>32</sup>T. Okamoto and I. Yamaguchi, *J. Phys. Chem. B* **107**, 10321 (2003).
- <sup>33</sup>G. W. Hanson, *IEEE Trans. Antennas Propag.* **56**, 747 (2008).
- <sup>34</sup>A. D. Phan, N. A. Viet, N. A. Poklonski, L. M. Woods, and C. H. Le, *Phys. Rev. B* **86**, 155419 (2012).
- <sup>35</sup>L. A. Falkovsky and S. S. Pershoguba, *Phys. Rev. B* **76**, 153410 (2007).
- <sup>36</sup>A. B. Kuzmenko, E. van Heumen, F. Carbone, and D. van der Marel, *Phys. Rev. Lett.* **100**, 117401 (2008).